Canadian Mineralogist
Vol. 27, pp. 499-507 (1989)

INTRACRYSTALLINE DISTRIBUTION OF MAJOR ELEMENTS IN ZONED GARNET FROM SKARN IN THE CHICHIBU MINE, CENTRAL JAPAN: ILLUSTRATION BY COLOR-CODED MAPS

TAKANORI NAKANO AND HIROYUKI TAKAHARA
Institute of Geoscience, University of Tsukuba, Tsukuba-shi, Tennoudai, Ibaraki 305, Japan

NORIMASA NISHIDA
Chemical Analysis Center, University of Tsukuba, Tsukuba-shi, Tennoudai, Ibaraki 305, Japan

ABSTRACT

Colored maps showing intracrystalline distribution Ca, Mn, Al, Fe, Mg and Ti in coexisting types of garnet from the Chichibu Fe–Zn–Cu–Pb mine, central Japan, have revealed a development of three or four growth zones. The composition of the garnet changes abruptly between zones. Calculations of garnet stoichiometry demonstrate a maximum substitution of 5% Mn in the dodecahedral site, up to 25% Ti + Mg in the octahedral site, and up to 4% Al in the tetrahedral site. Slight but distinct differences in mineral chemistry between the two types of garnet suggest that the skarn-forming fluid was locally heterogeneous during the metasomatic process, even on a scale of 200–1000 μm.

Keywords: colored compositional map, multiple elements, zoned garnet, skarn, stoichiometry, octahedral site, local heterogeneity, metasomatic process, Chichibu base-metal deposit, Japan.

SOMMAIRE

Des cartes coloriées servant à démontrer la distribution interne des éléments Ca, Mn, Al, Fe, Mg et Ti dans deux types de grenat coexistants dans la mine de Fe–Zn–Cu–Pb de Chichibu, dans la partie centrale du Japon, révèlent la présence de trois ou quatre zones de croissance. La composition du grenat change rapidement d'une zone à l'autre. Les calculs de la stoechiométrie du grenat révèlent jusqu'à 5% de Mn dans le site dodécaédrique, 25% de Ti + Mg dans le site octaédrique, et 4% de Al dans le site tétraédrique. De légères distinctions dans le chimisme des deux sortes de grenat font penser que la phase fluide responsable pour la formation du skarn n'était pas homogène au cours des réactions métasomatiques, même sur une échelle de 200–1000 μm.

(Traduit par la Rédaction)

Mots-clés: carte de composition en couleurs, éléments multiples, grenat zoné, skarn, stoechiométrie, site octaédrique, hétérogénéité locale, processus métasomatique, gisement de métaux de base de Chichibu, Japon.

INTRODUCTION

Extensive studies using the electron-probe microanalyzer (EPMA) have documented the existence of compositional heterogeneity in a wide variety of minerals. Elemental distributions in metamorphic garnet have been widely investigated (*e.g.*, Atherton 1976), as this mineral retains a chemical record of its growth history. In skarns, garnet is claimed to display compositional zoning between andradite and grossular (*e.g.*, Lessing & Standish 1973, Murad 1976). Several EPMA studies indicate the presence of Mn, Fe^{2+} and Mg in the dodecahedral site, Ti and Cr in the octahedral site, and Al in the tetrahedral site of the garnet structure (*e.g.*, Shimazaki 1977, Sato 1980, Einaudi & Burt 1982). Compositional mapping of such a multitude of elements in garnet from skarns is expected to provide constraints both on the structural site for cations and on the metasomatic process through which the garnet-bearing skarn evolved. Recent progress in EPMA has made it possible to draw a colored map showing element distribution within coarse-grained materials.

Coexisting zoned garnet crystals, each with a different internal texture, were discovered in the garnetiferous skarn of the Chichibu mine, central Japan. This study was undertaken to demonstrate the potential of color-coded compositional mapping of many elements (Al, Ca, Fe, Mg, Mn and Ti) in these zoned crystals.

SAMPLE DESCRIPTION

The Chichibu Fe–Cu–Zn–Pb mine, representative of skarn deposits in Japan, is located about 100 km WNW of Tokyo (Lat. 35° 50′N, Long. 138°50′E). The geology and skarn of this mine were described by Kitamura (1975) and Ishihara *et al.* (1987). The sample was collected from the garnet–clinopyroxene skarn, which replaced a crystalline limestone. The sample is composed of garnet, calcite, magnetite and clinopyroxene, with trace amounts of titanite, ilmenite and pyrite. The texture of this skarn is shown schematically in Figure 1. This figure shows that two types of garnet (1 and 2) are recognized on the basis of grain size, internal texture and crystal

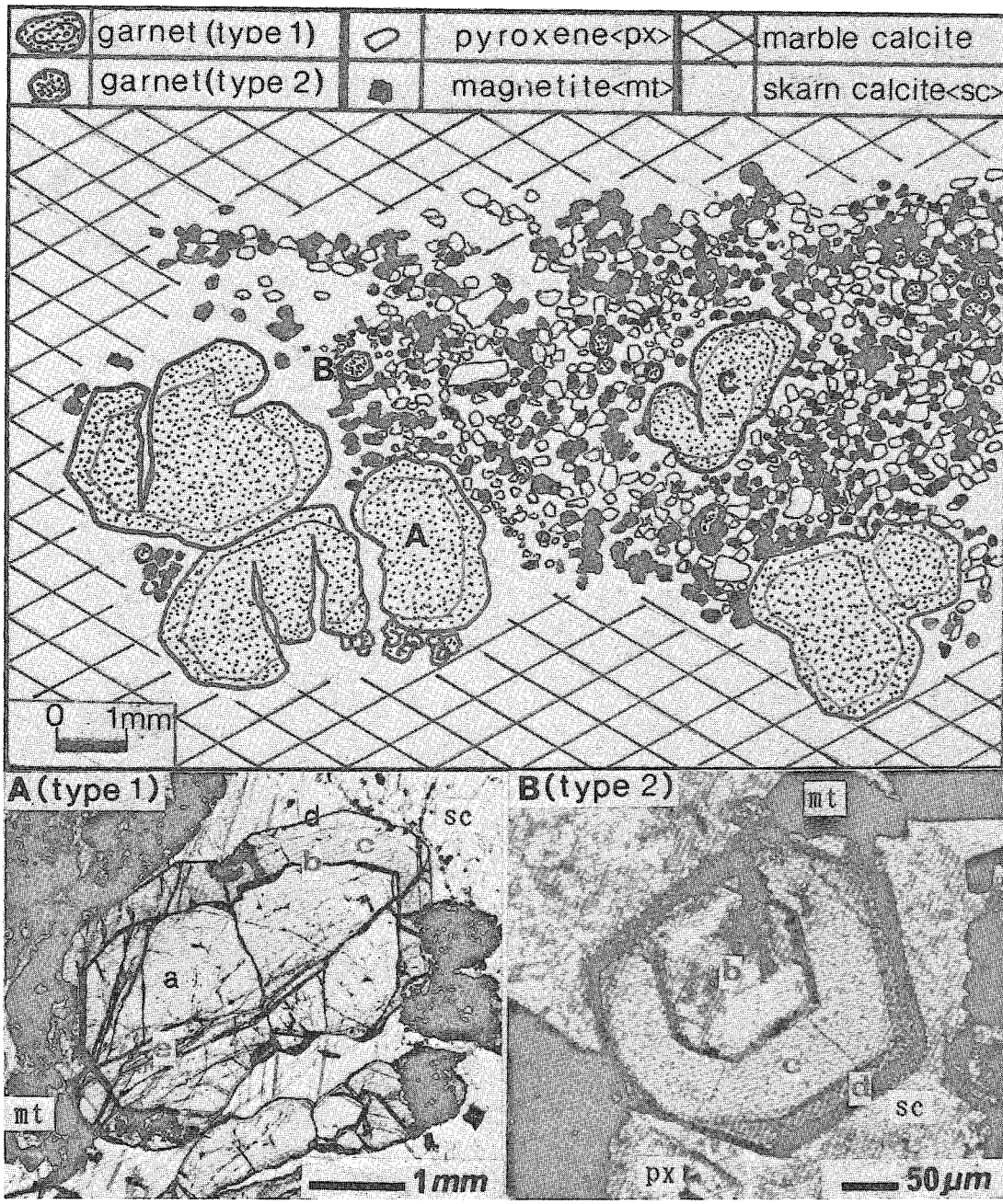

FIG. 1. Sketch of the thin section and microphotograph of two grains of garnet (grain A: type 1, and B: type 2) as seen under plane-polarized light. Location of grain C (subtype-1) also is shown in the sketch. Zonal arrangement (*a, b, c, d* and *e*) in the grains is shown in the photograph.

form. Microphotographs of the two types of garnet, used for the compositional mapping, are shown in Figure 1.

Garnet of type 1 has an ellipsoidal shape, measures 3–7 mm along a long axis and 2-4 mm along a short one, and shows four growth zones (*a, b, c*

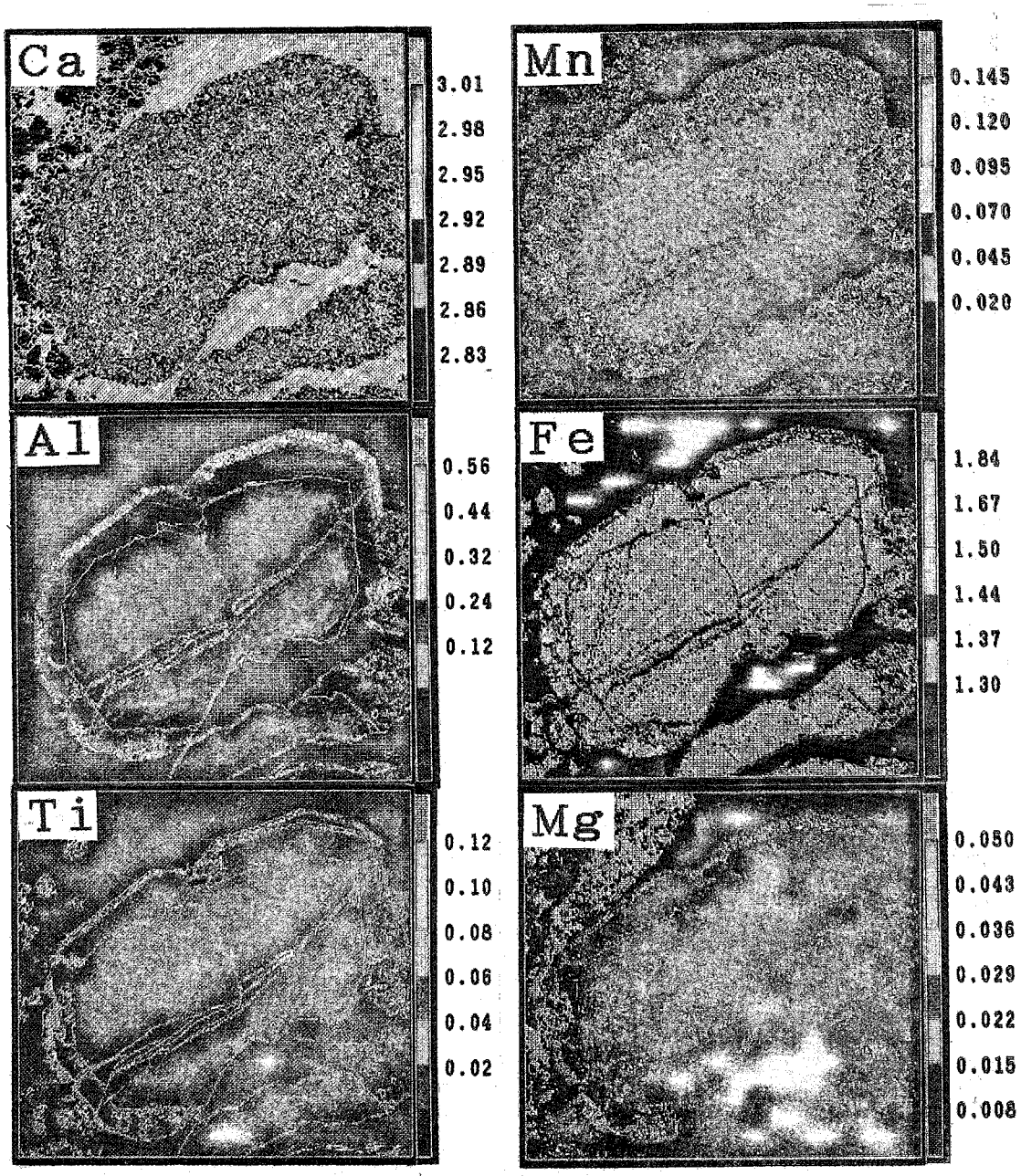

FIG. 2. Distribution map for elements Ca, Mn, Al, Fe, Ti and Mg in garnet of type 1.

and *d*) from core to rim. Garnet veins (zone *e*), occasionally cored by calcite, develop in zones *a* to *d*. Type-1 garnet is distinguished from type-2 garnet by the existence of zone *a*, which consists of a large core with a yellowish tint. An oscillatory zone having weak birefringence is locally observable adjoining zone *b*. Zone *b* is characterized by a narrow zone about 30 μm in width and by anomalous birefringence. Zone *c*, an isotropic zone with a brownish tint, is distinguished from zones *d* and *e*, which exhibit weak birefringence.

Garnet of type 2 has a dodecahedral habit, is 100–300 μm in diameter, and has three growth zones. The zones are named *b*, *c* and *d* from core to rim;

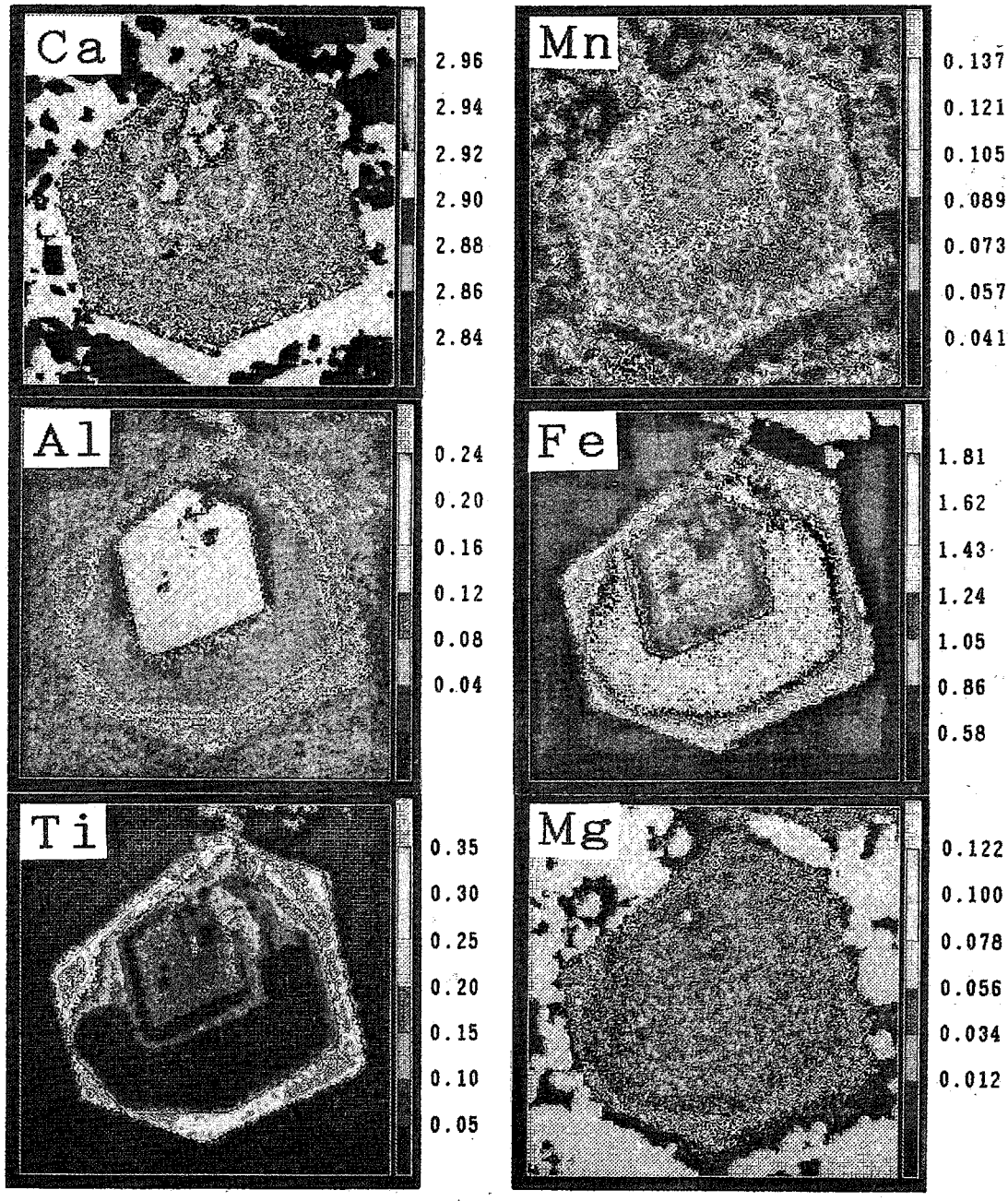

FIG. 3. Distribution map for elements Ca, Mn, Al, Fe, Ti and Mg in garnet of type 2.

based on the optical and compositional similarity to type-1 garnet, as described in a later section. Zone *b* is a colorless core and shows a strong birefringence, whereas zones *c* and *d* display a homogeneous isotropic character. The outermost zone, *d*, is characterized by its brown color. No zone corresponding to zone *a* in type-1 garnet is observable.

In general, grains of type-1 garnet are distributed along the contact with marble, whereas type-2 garnet occurs a small distance away from the marble.

However, some coarse grains, which are morphologically classified as of type 1, occur sparsely in an area of type-2 garnet (*e.g.*, grain C in Fig. 1); they have a zone *a* with a large core, whereas their zones *b*, *c* and *d* display the same optical and compositional character as type-2 garnet, as described later. We believe that this kind of garnet has an intermediate character between the two main types of garnet; it is thus classified as of subtype 1.

Magnetite and calcite, both of which show a euhedral shape and a range in grain size from 50 to 500 μm, occur as a matrix around the garnet grains (Fig. 1). All skarn minerals are interstitially surrounded by coarse-grained calcite termed skarn calcite, which is equigranular. Magnetite is partly included in or replaces type-2 garnet, the outer zones (*b*, *c* and *d*) of type-1 garnet and pyroxene, suggesting that magnetite crystallized after the formation of the zone *a* in type-1 garnet. However, there is no textural evidence of replacement of pyroxene or magnetite by garnet, suggesting that the garnet crystallized by replacement of calcite in the host marble.

Experimental

Chemical analyses of the garnet were carried out with a computer-controlled JEOL JXA-8621 supermicroprobe set up in the Chemical Analysis Center, University of Tsukuba. Quantitative analyses of garnet were done for selected points using an accelerating voltage of 15 kV and the OXIDE-ZAF correction program from JEOL. Concentrations of eleven elements (Al, Ca, Cr, Fe, K, Mn, Mg, Na, Ni, Si and Ti) were determined. Among these, Na, Cr and Ni contents were found to be present at trace levels ($<$ 0.07 wt.% Na_2O, Cr_2O_3, NiO), and K content was consistently below the limit of detection ($<$ 0.01 wt.% K_2O).

Compositional mapping was carried out for the seven remaining elements (Al, Ca, Fe, Mg, Mn, Si and Ti) using an accelerating voltage of 25 kV, a beam diameter of 5 μm and counting times of 150 ms for individual spots. A total of about 180,000 and 40,000 points were analyzed in crystals of type-1 and type-2 garnet, respectively.

Preparation of the Colored Maps

The colored maps were originally drawn by dividing X-ray intensities of each element into eight colored gradations. Therefore, individual gradation, strictly speaking, does not imply a range in the concentration of elements. Quantitative analyses for selected points make it possible to transform the gradation in the X-ray intensity of elements into their concentrations. Cation proportions were calculated on the basis of 12 oxygen atoms; we assumed that all the iron is Fe^{3+}.

Colored maps showing the distribution of six elements (Ca, Mn, Al, Fe, Ti and Mg) are shown in Figures 2 (type-1 garnet) and 3 (type-2 garnet). Color coding the concentration of each element in Figures 2 and 3 is done on the basis of atomic proportion. As described in the latter section, the concentration of each element in the garnet differs among zones and even within the same zone between the two types. However, some systematic substitutional relation among elements exists throughout zones. To illustrate such compositional relations more effectively on Figures 2 and 3, the scale for concentration is adjusted by elements and type of garnet. Some care is necessary, since the scale is not determined by dividing a whole range of concentration of each element in the garnet into the same interval. Therefore, the uppermost and lowermost concentration of the element is not shown in the two figures. For example, as the atomic proportion of Al is in a range from 0 to 0.848 for type-1 garnet and from 0 to 1.304 for type-2 garnet, the scale for the color coding of Al concentration is modified in the two garnets, 0.12 in the former and 0.04 in the latter, respectively; Al content of zone *b* in type-2 garnet, which covers a wide range, 0.24–1.304, is shown by only white coding.

Results and Discussion

Garnet composition within a single zone

Individual zones have a distinct composition. Definite compositional differences are not observed among garnet grains of the same type. Average compositions of each zone for type-1, type-2 and subtype-1 garnets is shown in Table 1. The composition of the clinopyroxene, which is homogeneous and diopsidic, also is shown in Table 1.

Garnet composition changes abruptly between zones, as well illustrated in Figures 2 and 3. The compositional pattern of Si (not shown) is constant among zones, except for zone *d* in type-2 garnet, which has a low Si content. The zones recognized microscopically (Fig. 1) are well reflected in the compositional pattern. For example, the anisotropic zones contain more Al and less Fe than the isotropic zones. That the birefringent zones have a high component of grossular has been recognized in other occurrences of grandite (*e.g.*, Lessing & Standish 1973, Murad 1976, Wada *et al.* 1978, Mariko & Nagai 1980).

The mineral chemistry of each zone is briefly described as follows. The innermost zone *a* in type-1 garnet is almost pure andradite, with 2–5% of the grossular component in the oscillatory birefringent zone. Zone *b* in the two types is characterized by the highest Al content (mole % grossular: 33–43 in type

TABLE 1. REPRESENTATIVE ANALYTICAL DATA FOR GARNET AND CLINOPYROXENE

Mineral	Garnet												Clino-
Type	1	sub-1	1	2	sub-1	1	2	sub-1	1	2	sub-1	1	pyroxene
Zone	a		b			c			d			e	
SiO_2	35.60	35.16	36.99	37.28	37.10	35.21	35.52	35.15	35.62	34.50	34.15	36.02	54.52
Al_2O_3	0.13	0.05	7.78	10.52	11.17	0.09	0.19	0.24	1.89	0.96	1.68	3.38	0.12
TiO_2	0.01	0.02	0.99	1.24	0.15	0.01	0.37	0.05	0.83	6.09	6.19	1.97	0.02
Fe_2O_3 *	30.15	30.45	19.50	15.60	15.85	30.44	30.40	30.89	26.92	23.09	22.16	24.02	2.26
Cr_2O_3	0.05	-	0.01	0.03	0.03	0.03	0.03	0.03	0.02	0.02	0.03	0.02	0.06
NiO	0.03	0.02	0.02	0.02	0.05	0.04	0.02	0.06	0.03	0.01	0.02	0.02	0.02
MnO	0.57	0.55	0.93	1.08	1.14	1.77	1.82	1.74	1.68	1.64	1.54	1.23	1.77
MgO	0.08	-	0.12	0.09	0.06	0.05	0.07	0.07	0.29	0.83	0.67	0.34	16.73
CaO	32.95	32.71	33.98	34.40	34.02	31.57	31.90	31.71	32.29	32.45	32.78	33.16	24.67
Total	99.59	98.96	100.33	100.27	99.57	99.20	100.34	99.94	99.57	99.59	99.22	100.17	100.17
						O = 12							O = 6
Si	3.020	3.006	2.986	2.970	2.975	3.009	2.999	2.985	2.995	2.888	2.864	2.976	1.993
Al	0.013	0.005	0.740	0.988	1.056	0.009	0.019	0.024	0.188	0.095	0.166	0.330	0.005
Ti	0.000	0.001	0.060	0.074	0.009	0.000	0.023	0.003	0.052	0.383	0.390	0.122	0.000
Fe	1.924	1.959	1.185	0.936	0.956	1.958	1.932	1.974	1.703	1.455	1.399	1.494	0.069
Cr	0.004	-	0.000	0.002	0.002	0.002	0.002	0.002	0.001	0.001	0.002	0.001	0.002
Ni	0.002	0.001	0.001	0.001	0.003	0.003	0.001	0.004	0.002	0.000	0.001	0.001	0.000
Mn	0.041	0.040	0.064	0.073	0.077	0.128	0.130	0.125	0.120	0.116	0.109	0.086	0.055
Mg	0.010	-	0.014	0.011	0.007	0.006	0.009	0.009	0.036	0.104	0.084	0.041	0.912
Ca	2.994	2.997	2.939	2.937	2.923	2.891	2.886	2.885	2.908	2.911	2.946	2.936	0.966
Total	8.008	8.010	7.991	7.991	8.009	8.005	8.001	8.012	8.006	7.953	7.962	7.989	4.003

* Total Fe was calculated as Fe_2O_3 for garnet and FeO for clinopyroxene.

1, 40–67 in type 2). Zone *c* resembles zone *a*, but contains more Mn and less Fe. Zone *d* is characterized by the highest Mg and Ti contents of all zones. Zone *e* has a similar composition to that of zone *d*. The compositional pattern, quantitative analytical data and textural observations seem to suggest that zone *e* was formed contemporaneously with or slightly later than zone *d* by the infilling of cracks in zones *a*, *b* and *c*. Therefore, we contend that the zonal arrangement from *a* through *b* and *c* to *d* and *e* corresponds to the successive growth-stages.

Garnet stoichiometry: Mg and Ti in the octahedral site

The coupled distributions of the pairs Ca–Mn and Fe–Al (Figs. 2, 3) suggest coupled substitutions involving Ca and Mn in the dodecahedral site and Fe and Al in the octahedral site. Data on the garnet give more reliable limitations on the site occupancies of the cations. The assumption of total Fe present as Fe^{3+} seems to be warranted, since a majority of cation totals fall in a narrow range 7.99-8.01 (Table 1). One exception occurs in zone *d* of type-2 and subtype-1 garnet, in which the cation total is slightly lower than in other zones and falls in a range around 7.96 (± 0.01). This shortfall may be explained by assuming an excess of Ti^{4+} in the octahedral site, as described later.

Although it is uncertain whether Ti substitutes in the tetrahedral site or the octahedral site, Huggins *et al.* (1977) established that the relative site-preference for the tetrahedral site must be in the order $Al > Fe^{3+} > Ti^{4+}$. As there are adequate amounts of Al and Fe^{3+} to fill the tetrahedral site, we can safely assume that Ti occupies the octahedral site. On the other hand, we assume that the dodecahedral site is occupied by cations of large ionic radius, such as Ca and Mn. An inverse correlation between Ca and Mn, and a total Ca + Mn in the range 2.975–3.075 (Fig. 4), demonstrate that this site is entirely occupied by these two cations. Excess Mn that cannot be accommodated in this site probably can be accommodated in the octahedral site. This hypothesis leads us to preclude the possibility of Mg in the dodecahedral site, since the ionic radius of Mg is smaller than that of Mn (Shannon & Prewitt 1969). Although Mg is generally assigned to the dodecahedral site as the pyrope component, Mg and Ti in this type of garnet may be accommodated in the octahedral site as the coupled substitution $Mg^{2+} + Ti^{4+} = R^{3+}$. Sympathetic patterns of Mg and Ti codistribution (Figs. 2, 3) can be ascribed to this kind of substitution scheme.

If the dodecahedral and octahedral sites are fully filled by the cations mentioned above, then the following two relations must apply. The first concerns cations in the octahedral site. As Ni and Cr can be

neglected as trace constituents, the relation is expressed by:

$$Fe + {}^{VI}Al + Ti + Mg + {}^{VI}Mn = 2.00$$

This relation is illustrated in Figure 5. The second relationship concerns charge balance. If it is assumed that Mn in the octahedral site is present as Mn^{2+}, not as Mn^{3+}, as is generally proposed, then the relation is expressed by:

$${}^{VI}Ti^{4+} = {}^{IV}Al^{3+} + {}^{VI}Mg^{2+} + {}^{VI}Mn^{2+}$$

This relation is also illustrated in Figure 6. In this figure, compositions of zone-*d* garnet of type 2 plot in a region of slight excess in Ti, which is consistent with the view that the total number of cations in this zone is slightly below 8.000. The degree of replacement by Al in the tetrahedral site, Mg + Ti in the octahedral site and Mn in the dodecahedral site attains up to 4%, 25% and 5%, respectively.

We have reached no definite conclusion as to the unusual scheme of substitution proposed for Mg. Garnet of high pyrope content is known to occur in rocks formed at high pressures and temperatures, such as a kimberlite or a mantle xenolith, and to contain appreciable amounts of Cr and an almandine component (*e.g.*, Deer *et al.* 1982). On the other hand, the pressure of formation of the Chichibu deposit is estimated to be low (around 0.5 kbar) using the sphalerite geobarometer (Shimizu & Shimazaki 1981). Relatively low pressures of formation and temperatures generally assumed to be around 300–500°C or the negligible content of Cr or Fe^{2+} in the garnet (or both) may favor the incorporation of Mg in the octahedral site.

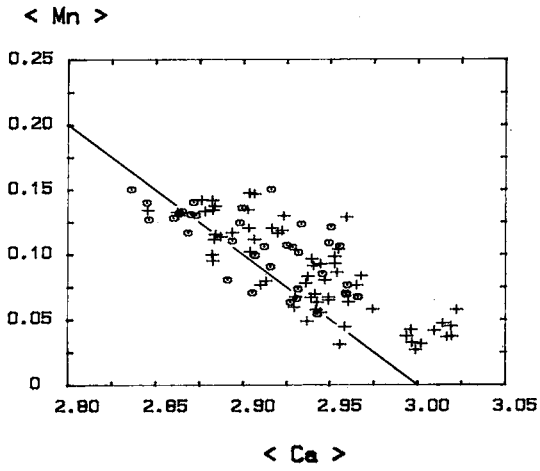

FIG. 4. Relation between Mn and Ca in the garnet. Solid line represents a 1:1 substitution between Mn and Ca in the dodecahedral site. Correlation coefficient between Mn and Ca is -0.80.

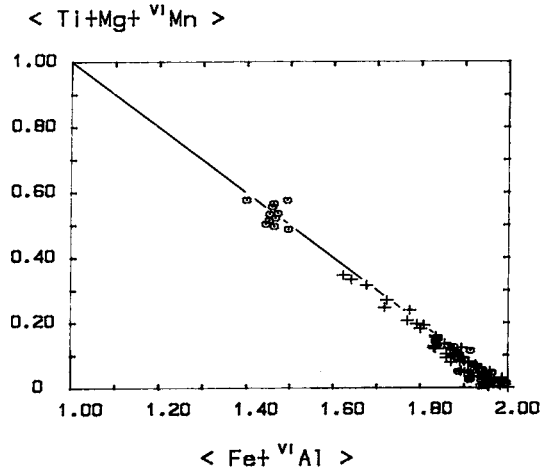

FIG. 5. Relation between ${}^{VI}Al + Fe^{3+}$ and $Ti + Mg + {}^{VI}Mn$ in the octahedral site. Solid line represents a 1:1 substitution between $({}^{VI}Al + Fe^{3+})$ and $(Ti + Mg + {}^{VI}Mn)$. Symbols are the same as in Figure 4.

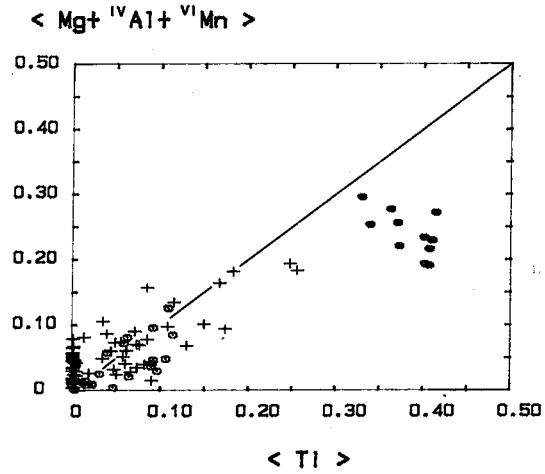

FIG. 6. Plot demonstrating $Ti^{4+} = {}^{IV}Al^{3+} + Mg + {}^{VI}Mn^{2+}$ to maintain the charge balance in the garnet. Solid circles represent compositions in zone *d* of type-2 garnet. Other symbols are the same as in Figure 4.

Compositional difference between the two types of garnet

Although the garnet chemistry varies more or less within an individual zone, similar compositional trends are observed throughout the same zones in both types (Table 1). The trends are well depicted on the Mn/(Mn + Ca) *versus* Fe/(Fe + Al + Mg + Ti) diagram (Fig. 7). As there is no cross-cutting relation between the two types of garnet, each zone (*b*, *c* and *d*) in both types seems to have crystallized

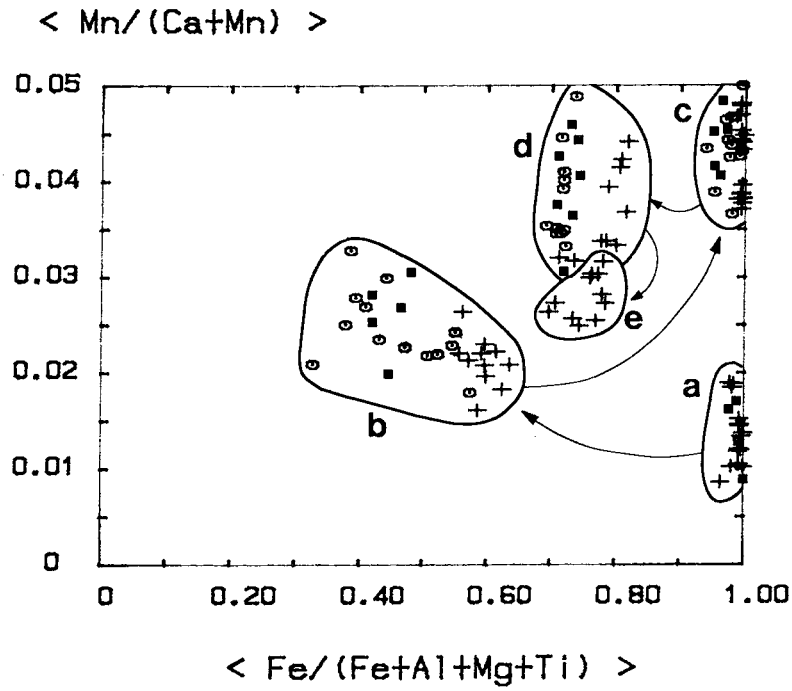

FIG. 7. Relation between Mn/(Mn + Ca) and Fe/(Fe + Al + Mg + Ti) in the individual zones (*a, b, c, d* and *e*) of the garnet. Arrows represent the direction of growth of the garnet. Symbols are the same as in Figure 4. Solid squares represent compositions in grain C of subtype-1 garnet.

almost simultaneously. Type-2 garnet may therefore have begun to crystallize after the formation of zone *a* in type-1 garnet.

The same zone in the two types of garnet has a slightly different composition (Fig. 7, Table 1). For example, Fe and Ti contents of the type-1 garnet are higher in all zones than in those of type 2. Such compositional differences suggest that the associated fluid chemistry may have been locally heterogeneous during the replacement reaction from calcite to garnet. This proposal is supported by the composition of subtype-1 garnet: zone *a* of subtype-1 garnet has a composition similar to that of zone *a* of type-1 garnet, whereas the composition of zones *b*, *c* and *d* is almost identical to that of the same zones of type-2 garnet. It thus appears that the composition of the garnet-forming fluid was homogeneous on the scale of a thin section during the formation of zone *a*, whereas it was locally heterogeneous even over a distance of 200–1000 μm (Fig. 1) between both types of garnet during the formation of zones *b*, *c* and *d*. Although many factors [fluid chemistry, $f(O_2)$, $f(CO_2)$ and temperature] may have affected garnet composition, we cannot specify at present which factors exerted a controlling influence.

However, considering the textural evidence that the garnet replaced host-marble calcite, it is evident that major elements in the garnet excluding Ca were derived from exotic fluids. A coexisting clinopyroxene rich in the diopside component does not necessarily demand a low Fe/Mg value in the metasomatic fluid. Negligible ferrous iron content in the garnet suggests that the metasomatic fluid had a high Fe^{3+}/Fe^{2+} value throughout the entire growth of the garnet. Therefore, it seems probable that the abrupt compositional changes between zones in the garnet are concomitant with changes in the skarn-forming fluid at conditions of elevated Fe^{3+}/Fe^{2+}.

A colored map showing the distribution of multiple elements within a mineral provides a powerful tool, not only to provide constaints on the growth history of the mineral, but also to deduce the likely structural sites of cations.

ACKNOWLEDGEMENTS

The authors express thanks to Professor T. Fujii, University of Tsukuba, for his encouragements throughout this study. We also acknowledge Dr. H. Yurimoto for giving us constructive advice on the

mineral chemistry of garnet. We wish to express our grateful thanks to Dr. R. F. Martin for his helpful advice and critical reading of the manuscript.

References

ATHERTON, M.P. (1976): Crystal growth models in metamorphic tectonics. *R. Soc. London, Phil. Trans.* **A283**, 255-270.

DEER, W.A., HOWIE, R.A. & ZUSMANN, J. (1982): *Rock-Forming Minerals. 1A. Orthosilicates* (Second ed.). Longman, London.

EINAUDI, M.T. & BURT, D.M. (1982): Introduction - Terminology, classification, and composition of skarn deposits. *Econ. Geol.* **77**, 745-754.

HUGGINS, F.E., VIRGO, D. & HUCKENHOLZ, H.G. (1977): Titanium-containing silicate garnets. I. The distribution of Al, Fe^{3+}, and Ti^{4+} between octahedral and tetrahedral sites. *Am. Mineral.* **62**, 475-490.

ISHIHARA, S., TERASHIMA, S. & TSUKIYAMA, K. (1987): Spatial distribution of magnetic susceptibility and ore elements, and cause of local reduction on magnetite-series granitoids and related ore deposits at Chichibu, central Japan. *Min. Geol.* **37**, 15-28.

KITAMURA, K. (1975): Al–Fe partitioning between garnet and epidote from the contact metasomatic copper deposits of the Chichibu mine, Japan. *Econ. Geol.* **70**, 725-738.

LESSING, P. & STANDISH, R. P. (1973): Zoned garnet from Crested Butte, Colorado. *Am. Mineral.* **58**, 840-842.

MARIKO, T. & NAGAI, Y. (1980): Birefringence and composition of grandite garnet from the Shinyama ore deposit of the Kamaishi mine, Iwate Prefecture, Japan. *Mineral. J.* **10**, 181-191.

MURAD, E. (1976): Zoned, birefringent garnets from Thera Island, Santorini Group (Aegean Sea). *Mineral. Mag.* **40**, 715-719.

SATO, K. (1980): Tungsten skarn deposit of the Fujigatani mine, southwest Japan. *Econ. Geol.* **75**, 1066-1082.

SHANNON, R. D. & PREWITT, C. T. (1969): Effective ionic radii in oxides and fluorides. *Acta Crystallogr.* **B25**, 925-946.

SHIMAZAKI, H. (1977): Grossular–spessartine–almandine garnets from some Japanese scheelite skarns. *Can. Mineral.* **15**, 74-80.

SHIMIZU, M. & SHIMAZAKI, H. (1981): Application of the sphalerite geobarometer to some skarn-type deposits. *Miner. Deposita* **16**, 45-50.

WADA, N., HIROWATARI, F. & TAKANO, Y. (1978): Optical properties, twin point groups and chemical compositions of anisotoropic garnets. *J. Mineral. Soc. Japan* **13**, 380-398 (in Japanese).

Received October 12, 1988, revised manuscript accepted February 28, 1989.